Invalidation Analysis and Revision of Polar Format Algorithm for Dechirped Echo Signals in ISAR Imaging

Yang Liu*, **Na Li, Bin Yuan, and Zengping Chen**

Abstract—In this paper, we present a detailed analysis on the invalidation of the polar format algorithm (PFA) for the dechirped echo signals in inverse synthetic aperture radar (ISAR) imaging. After the data-driven translational motion compensation, the polar section of the dechirped signals is often undermined, and then the PFA is invalid. A revision method by range shifting is proposed to compensate the echo signals, and the standard polar section is obtained. An improved performance was achieved on the simulated and real data experiments. The theoretical analysis and the proposed method are confirmed.

1. INTRODUCTION

Inverse synthetic aperture radar (ISAR) can generate 2D images for a non-cooperative moving target in military and civilian applications. The high range resolution is proportional to the bandwidth of the transmitted signal. The high cross-range resolution is achieved using a synthetic antenna aperture generated by the rotational motion of the target [1]. The range resolution ρ_r is defined as $\rho_r = c/(2B)$, where c is the light velocity, B is the signal bandwidth. The cross-range resolution ρ_a is defined as $\rho_a = \lambda/(2\Theta)$, where λ is the signal wavelength, and Θ is the target rotation angle within the coherent processing interval (CPI).

Generally, in a traditional ISAR imaging system, a linear frequency modulation (LFM) signal is transmitted, and the echo signals are then dechirped to decrease the receiver bandwidth. Several popular ISAR signal processing algorithms are proposed in the literatures, such as the Range-Doppler algorithm (RDA) [2], the Keystone algorithm [3, 4] and the polar format algorithm (PFA) [5–7]. The RDA is applicable when the rotation angle is small to ensure there is no significant migration through range cells (MTRC) and time-varying Doppler in the echoed signal. The Keystone algorithm is effective for the migration through range resolution cells (MTRRC) caused by the target rotation with constant velocity. However, it is invalid for the migration through cross-range resolution cells (MTCRRC). The PFA was first used to compensate the MTRC in SAR imaging [5]. It was introduced in ISAR imaging later. The PFA algorithm firstly interpolates the observed signal from polar sector support region to the Cartesian rectangular region. The fast Fourier transform (FFT) is followed to focus the ISAR image [8, 9]. Since both the range and the Doppler curve are permitted in the PFA, the maximum rotation angle is significantly wider for the PFA algorithm compared to the Keystone and the RDA.

In practical applications, the PFA requires accurate estimation of the rotation parameter to interpolate the complex data points. However, once the translational motion is compensated, the polar section of the dechirped signals is often undermined, since the rotation center (RC) is deviated from the reference range. In that case, the PFA is invalid. This paper first analyzes the PFA algorithm and the factors causing the invalidation detailedly. Then we propose a method to revise the polar sector of the echoes. The PFA algorithm is applied to the revised signal in order to obtain a focused imaged. Experimental results were carried on both of the simulated and real data to demonstrate the accuracy of the analysis and the effectiveness of the improved method.

* Corresponding author: Yang Liu (liuyangjiangxi@163.com).
The authors are with the Automatic Target Recognition (ATR) Laboratory, China.

The rest of the paper is organized as follows. The dechirped echo signals and polar format algorithm are introduced in Section 2. Section 3 analyzes the invalidation of the PFA algorithm in ISAR imaging for dechirped signal and presents an improved PFA. Experimental results and analysis are reported in Section 4, followed by conclusions in Section 5.

2. DECHIRPED ECHO SIGNALS AND PFA ALGORITHM

2.1. Dechirped Signal Model Formulation

The point scatterer model is commonly used in radar imaging systems [9]. If the translational motion has been fully removed, the geometry of radar imaging is depicted in Fig. 1. The instantaneous distance from the scattering point p_k with position (x_k, y_k) to the radar can be approximated as:

$$R_k(t) \simeq r_a(t) + x_k \sin \theta(t) + y_k \cos \theta(t) \tag{1}$$

where r_a is the range from target RC to the radar, and $\theta(t)$ is the instantaneous rotation angel at arbitrary time.
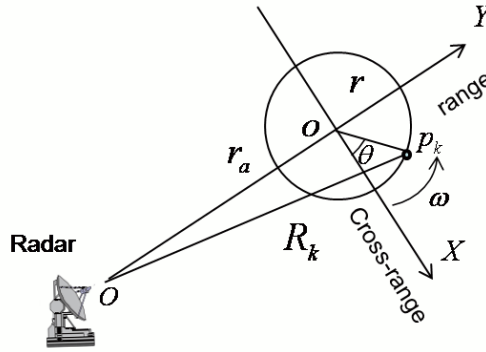
Figure 1. Geometry of the scattering point p.

In an ISAR imaging system, a LFM signal is often transmitted, and then the echo is dechirped to reduce the receiver bandwidth. Supposing that the target consists of K point scatterers, the return signals can be expressed as:

$$
\begin{aligned}
s_R\left(\hat{t}, t_m\right) = &\sum_{k=1}^{K} \sigma_k \text{rect}\left\{\left[\hat{t} - \left(2R_k\left(t_m\right)/c\right)\right]/T_p\right\} \\
&\exp\left\{-j2\pi\left(f_c\left(\hat{t} - \left(2R_k\left(t_m\right)/c\right)\right) + \frac{1}{2}\gamma\left(\hat{t} - \left(2R_k\left(t_m\right)/c\right)\right)^2\right)\right\}
\end{aligned} \tag{2}
$$

where σ_k, c and f_c are the backward scattering coefficient, light speed and carrier frequency, respectively. γ denotes the chirp rate of the transmitted signal. Since the target motion is much lower than the speed of light, the full time $t = \hat{t} + t_m$ is expressed in the form of fast time $\hat{t}$ and slow time $t_m = mT_p$, where m are integers and T_p denotes the pulse width. Suppose that the reference point (RP) is o and its range to radar is $r_0(t)$. Then after the dechirping, the received signal is given as:

$$
\begin{aligned}
s_{R2}\left(\hat{t}, t_m\right) = &\sum_{k=1}^{K} \sigma_k \text{rect}\left\{\left[\hat{t} - \left(2\left(R_k\left(t_m\right) - r_0\left(t_m\right)\right)/c\right)\right]/T_p\right\} \\
&\exp\left\{j\frac{4\pi}{c}\left(f_c + \gamma\left(\hat{t} - 2R_0\left(t_m\right)/c\right)\right)R_{ps\_k}\left(t_m\right)\right\}\exp\left(j\psi_k\left(t_m\right)\right)
\end{aligned} \tag{3}
$$

where

$$R_{ps\_k}\left(t_m\right) = R_k\left(t_m\right) - r_0\left(t_m\right), \quad \psi\left(t_m\right) = \frac{4\pi\gamma}{c^2}R_{ps\_k}^2\left(t_m\right) \tag{4}$$

$R_{ps\_k}(t_m)$ is the instantaneous range from P_k to o, and $\psi(t_m)$ is the residual video phase (RVP). Generally, the RVP can be removed easily, when dealing with small targets.

Let us denote $f = \gamma\left(\hat{t} - 2r_0\left(t_m\right)/c\right)$ and substitute it into (3), and then one can obtain:

$$s_{R3}(f, t_m) = \sum_{k=1}^{K} \sigma_k \text{rect}\left\{\frac{(f/\gamma) - (2\left(R_k\left(t_m\right) - r_0\left(t_m\right)\right)/c)}{T_p}\right\} \exp\left\{j\frac{4\pi}{c}\left(f_c + f\right) R_{ps\_k}\left(t_m\right)\right\} \quad (5)$$

Assume that the RP locates at the RC, i.e., $r_0(t) = r_a(t)$, then one can obtain R_{ps_k} from (1):

$$R_{ps\_k} \simeq x_k \sin\theta(t) + y_k \cos\theta(t) \quad (6)$$

Since $R_k\left(t_m\right) \simeq r_0\left(t_m\right)$ for small targets, the dechirped echo signals can be finally expressed as:

$$s_{R4}(f, \theta) = \sum_{k=1}^{K} \sigma_k \text{rect}\left\{\frac{f}{B}\right\} \exp\left\{j\frac{4\pi}{c}\left(f_c + f\right)\left(x_k \sin\theta(t) + y_k \cos\theta(t)\right)\right\} \quad (7)$$

where $B = \gamma T_p$ denotes the signal bandwidth.

2.2. Polar Format Algorithm for Dechirped Signals

Since both the range and Doppler curve are permitted in the PFA, the maximum rotation angles for the PFA algorithm are wider. Let $K_R = -(4\pi/c)(f_c + f)$, then the phase term of (7) can be expressed as:

$$\Phi(\theta) = K_R(x_k \sin\theta + y_k \cos\theta) = K_x x_k + K_y y_k \quad (8)$$

where (θ, K_R) is the polar format of (K_x, K_y) in a Cartesian coordinate system. If the target rotation angle Θ is known, the target image can be reconstructed from 2D Fourier Transform (2D-FT). However, the FT algorithm requires a rectangular raster distribution of the data points, and the signal model can acquire a sector support region. Therefore, interpolation of the observed signal on a polar sector support region to a Cartesian rectangular system is required. As it is shown in Fig. 2, the radial wavenumber K_R satisfies:

$$K_R \in [K_{R1}, K_{R2}] = \frac{4\pi}{c}\left[f_c - \frac{B}{2}, f_c + \frac{B}{2}\right] \quad (9)$$

The azimuth wavenumber is $(4\pi/\lambda) \cdot \Theta$.

An illustration of the PFA algorithm is shown in Fig. 3. If $K_{R2}\cos\Theta \leq K_{R1}$, the interpolation error will increase with Θ increasing, which results in a large vacant space in the wavenumber spectrum filled with stripe in the Fig. 3. Then, the maximum rotation angle for PFA is:
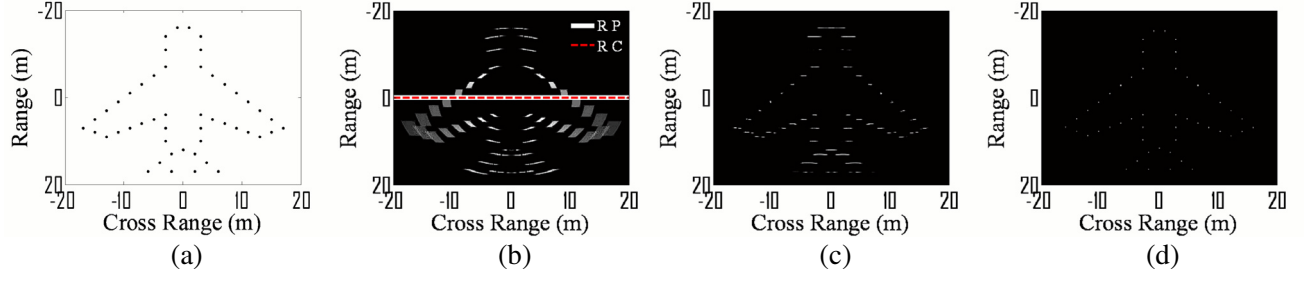
$$\Theta_{PFA} = 2\cos^{-1}\frac{K_{R1}}{K_{R2}} = 2\cos^{-1}\frac{1 - 0.5\mu}{1 + 0.5\mu} \quad (10)$$
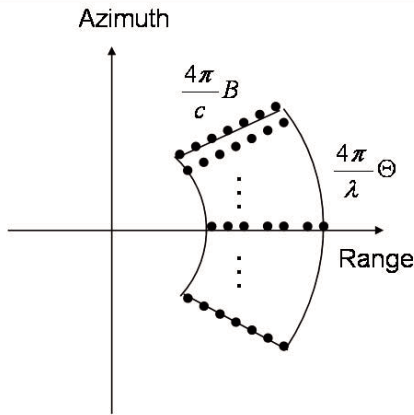
Figure 2. Wavenumber spectrum of echo signals after de-chirping.
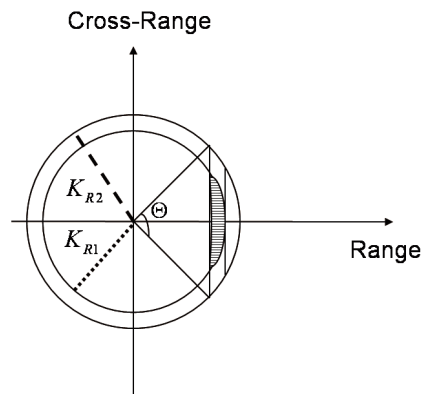
Figure 3. Wavenumber spectrum for $K_{R2}\cos\Theta \leq K_{R1}$.

Figure 4. Imaging results of a simulated aircraft with the rotation center being the same as the reference point. (a) Scatterers model. (b) RD image. (c) Image after Keystone transform. (d) Image after PFA.

where $\mu = B/f_c$. According to (10), Θ_{PFA} is merely a function of independent of the target size and the range resolution. Therefore, Θ_{PFA} is much larger than Θ_{RD} and $\Theta_{Keystone}$. The ISAR images for a simulated aircraft are presented in Fig. 4. The aircraft is composed of 49 point caterers with equal reflectivity. The size of the aircraft shown in Fig. 4(a) is $20\,\text{m} \times 20\,\text{m}$. The radar transmits LFM signals with a carried frequency of $15\,\text{GHz}$ and a bandwidth of $2\,\text{GHz}$. The range resolution $\rho_r = 0.075$. In order to obtain high cross-range resolution matched with the range resolution, the target coherent rotation angel is set to $\Theta = 0.1\,\text{rad}$ and the rotational velocity is set to $\omega = 0.05\,\text{rad/s}$. The RC and RP are both located at $(0\,\text{m}, 0\,\text{m})$ in the target coordinate system. The time of coherent processing interval is $T_{CPI} = 2\,\text{s}$, the pulse number is $M = 1024$, and the pulse repetition frequency (PRF) is $1000\,\text{Hz}$. Meanwhile, the number of range bins in high resolution range profile (HRRP) is $N = 1024$.

Figure 4(b) shows the ISAR image achieved by the RDA algorithm without any compensation. The blurring effects caused by the MTRC can be found in both of the range cell and Doppler cell. The obtained ISAR image using the Keystone algorithm is shown in Fig. 4(c). It can be seen that the blurring in range cells caused by MTRRC is compensated, but the blur in Doppler cells still remains. Fig. 4(d) presents the ISAR image obtained by the PFA algorithm, where the target scatterers are optimally focused.

3. ANALYSIS OF PFA AND THE IMPROVED METHOD

3.1. Analysis and Simulation of the Invalidation of the PFA

According to (6) and (7), when the RC is located at the cell of the RP, the phase term of the dechirped signals can be expressed in polar format. Thus we can use the standard PFA algorithm to obtain a focused ISAR image without MTRC, as it is shown in Fig. 4. However, in practical applications, the RC is not always the same as the RP. Assume that the distance of $r_0(t)$ and $r_a(t)$ is $\Delta r = r_a(t) - r_0(t)$, (6) and (7) can be expressed as follows:

$$R'_{ps\_k} \simeq \Delta r + x_k \sin\theta(t) + y_k \cos\theta(t) \tag{11}$$

$$s'_{R4}(f,\theta) = \sum_{k=1}^{K} \sigma_k \text{rect}\left\{\frac{f}{B}\right\} \exp\left\{j\frac{4\pi}{c}(f_c + f)(\Delta r + x_k \sin\theta(t) + y_k \cos\theta(t))\right\} \tag{12}$$

Then, the phase term of (7) can be expressed as:

$$\Phi(\theta) = K_R(\Delta r + x_k \sin\theta + y_k \cos\theta) = K_R\Delta r + K_x x_k + K_y y_k \tag{13}$$

where $K_R = -(4\pi/c)(f_c + f)$.

Equation (13) indicates that the disturbed phase term $K_R\Delta r$ can cause the performance degradation when the PFA algorithm is applied. For clarity, we provide some simulation results in Fig. 5 to indicate the degradation of PFA image from the imprecise RC. The target is the one in Fig. 4. The new given dechirped signals in Fig. 5 have the RC highlighted by red dashed, at $(0\,\text{m}, 10\,\text{m})$ in the target coordinate system. The RP is highlighted by the white solid line in Fig. 5(a), locating at
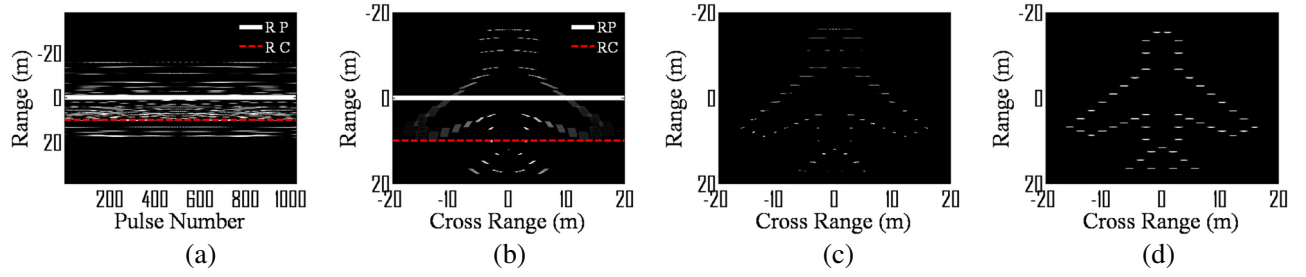
Figure 5. Analysis of the PFA algorithm. (a) HRRPs of the simulated aircraft. (b) Image by RDA. (c) Image after Keystone transform. (d) Image by traditional PFA.

$(0\,\text{m}, 0\,\text{m})$. The ISAR image achieved by the RDA is shown in Fig. 5(b) and the imaging result achieved with the PFA algorithm is shown in Fig. 5(d). Compared to the image in Fig. 4(d), the blur in Fig. 5(b) was not fully overcome by PFA.

3.2. The Improved PFA Algorithm

According to the theoretical analysis of the PFA algorithm, if the RC on slant range is not overlapped with the RP, the MTCRRC in ISAR imaging cannot be compensated using the PFA algorithm. In order to resolve this problem, the dechirped signals after translational compensation are shifted in slant range, and the RC is located at the center of the HRRP. As a result, the shifted signals follow the standard polar format.

It is known that the RP is located at the center of the HRRP. Therefore, the location of RC in HRRP is $r'_a(t) = \Delta r = r_a(t) - r_0(t)$. When the estimation value $\Delta\tilde{r}$ of Δr is obtained, $s'_{R4}(f,\theta)$ is shifted in the slant range, and the new dechirped signals $s_{R5}(f,\theta)$ can be written as:

$$
s_{R5}(f,\theta) = s'_{R4}(f,\theta) \cdot \exp\left\{-j\frac{4\pi}{c}(f_c + f)\Delta\tilde{r}\right\}
$$
$$
= \sum_{k=1}^{K} \sigma_k \text{rect}\left\{\frac{f}{B}\right\} \exp\left\{j\frac{4\pi}{c}(f_c + f)\left[(\Delta r - \Delta\tilde{r}) + (x_k \sin\theta(t) + y_k \cos\theta(t))\right]\right\} \quad (14)
$$

If the value of $\Delta\tilde{r}$ is equal to Δr, then $\Delta r - \Delta\tilde{r} \simeq 0$. The shifted signals in (14) become:

$$
s_{R5}(f,\theta) = s'_{R4}(f,\theta) \cdot \exp\left\{-j\frac{4\pi}{c}(f_c + f)\Delta\tilde{r}\right\}
$$
$$
= \sum_{k=1}^{K} \sigma_k \text{rect}\left\{\frac{f}{B}\right\} \exp\left\{j\frac{4\pi}{c}(f_c + f)(x_k \sin\theta(t) + y_k \cos\theta(t))\right\} \quad (15)
$$

From formula (15), the shifted signals have the same format as (7). $s'_{R4}(f,\theta)$ is revised to standard polar format. When the PFA algorithm is performed on the revised signals $s_{R5}(f,\theta)$, the MTRC of $s'_{R4}(f,\theta)$ is compensated. Note that in Eq. (14), the RC should be estimated firstly. Many approaches have been proposed in the literatures for the RC estimation in ISAR imaging [10–14]. Here, we utilize the integrated cubic phase function (ICPF) to estimate rotation motion information. The ICPF extends the CPF and provides improved estimation performances of multi-component linear frequency modulated signals [11]. Fig. 6 shows the estimation coefficient of quadratic phase along the slant-range using ICPF. The RC is located at the range of $10.1\,\text{m}$, since the absolute value of the quadratic phase coefficient is minimized.

As shown in Fig. 7(a), the RC was shifted to the center of the HRRPS according to the estimated RC in Fig. 6. Taking PFA on the shifted signals, the compensated ISAR image is obtained in Fig. 7(b). It can be seen that the invalidation of the dechirped signals in Section 3 was revised, and the image was well focused, since the MTRC was fully compensated.
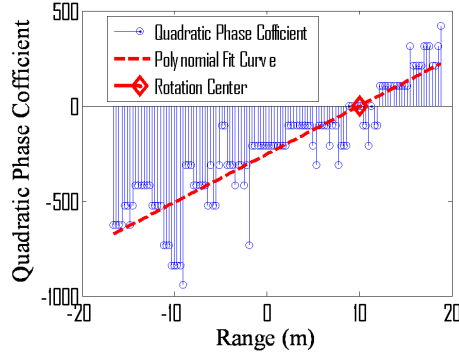
Figure 6. Coefficient of quadratic phase estimated by ICPF method.
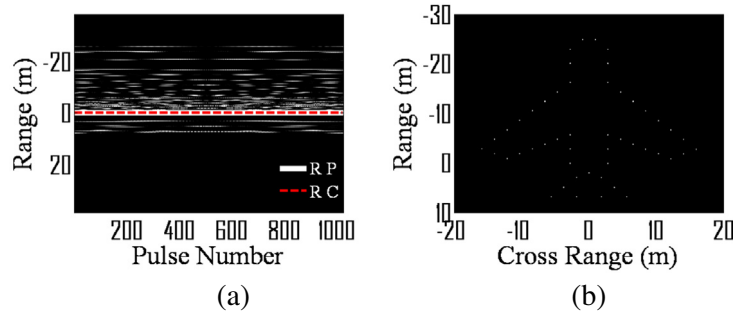
Figure 7. The results of the revised PFA in Fig. 5. (a) HRRPs after range shift. (b) Image after revised PFA.

## 4. EXPERIMENT AND PERFORMANCE ANALYSIS

In the first experiment, simulated data of aircraft (MIG-25) [1] were used. The aircraft is composed of 120 point scatterers with equal reflectivity. The radar transmits LFM signals with a carried frequency of 9 GHz and a bandwidth of 512 MHz. It was assumed that the aircraft had rotational motion only.

Figure 8(a) shows the image obtained by using RDA without any compensation, where the blurring effects caused by the MTRC are significant. The RC is located at -4.1 m, which is estimated by ICPF in Fig. 8(g) and highlighted by the dashed line in Fig. 8(c). Fig. 8(b) presents the ISAR image after MTRRC compensation, where the slant range migration has been corrected, and the cross range migration can still be found. As shown in Fig. 8(d), since the RC was not located at the same position as the RP, the image after PFA was still blurred. With the proposed ICPF estimation of RC, the HRRPS of shifted signals are shown in Fig. 8(e), and the image after PFA interpolating is shown in Fig. 8(f), where the MTRC was fully compensated.

Figure 9 depicts the ISAR image entropy [15] and contrast [16] after PFA interpolating with different shift range. The more focused the image is, the smaller the entropy is, and the larger the contrast is. The minimized entropy and the maximized contrast are achieved when the shift range is -4.1 m. It illustrates that more closed between the shift range and RC, more focused the compensated ISAR image is and consequently the more efficient the PFA is.

In the second experiment, the real data provided by ATR National Defense Science and Technology Key Laboratory were used. The data were collected by ground-based imaging radar. The target is a stably flying airplane of Boeing 737, whose model is shown in Fig. 10(a). The carrier frequency is 10 GHz and the bandwidth is 1 GHz.

The translational compensation was firstly carried on the echoes and the aligned profiles are shown in Fig. 10(b). By using the ICPF algorithm, the estimated rotation angle is 8.03° and the RC is located at -15 m in Fig. 10(c). For comparison, the RDA, Keystone algorithm and traditional PFA were carried on the data in Fig. 10(b), and the images are shown in Figs. 10(d)–(f). From Fig. 10(d), the blurring
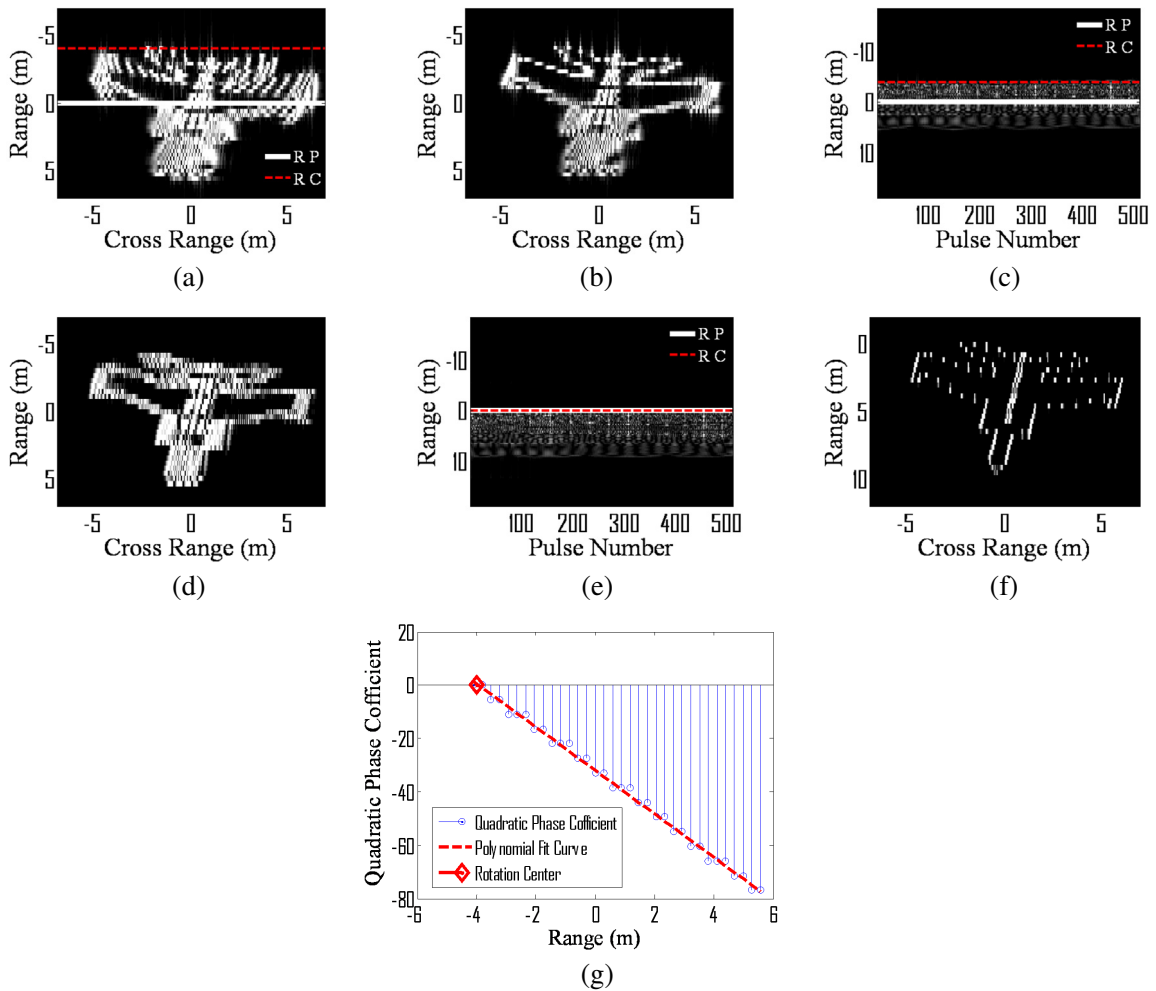
Figure 8. Simulated experiment of MIG-25. (a) RD image. (b) ISAR image after MTRRC. (c) Original HRRPs. (d) ISAR image after PFA. (e) HRRPs after range shift. (f) ISAR image of shifted signals after PFA. (g) Coefficient of quadratic phase estimated by ICPF method.
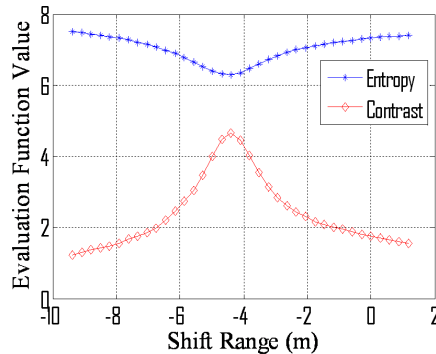
Figure 9. The entropy and contrast of the image after PFA with different shifted ranges.

effects caused by MTRC in both of the range and Doppler cell can be found in the RD image. The image using the Keystone algorithm in Fig. 10(e) illustrates that the MTRC in slant-range dimension is compensated but the blur in the Doppler dimension still remains. As shown in Fig. 10(f), when
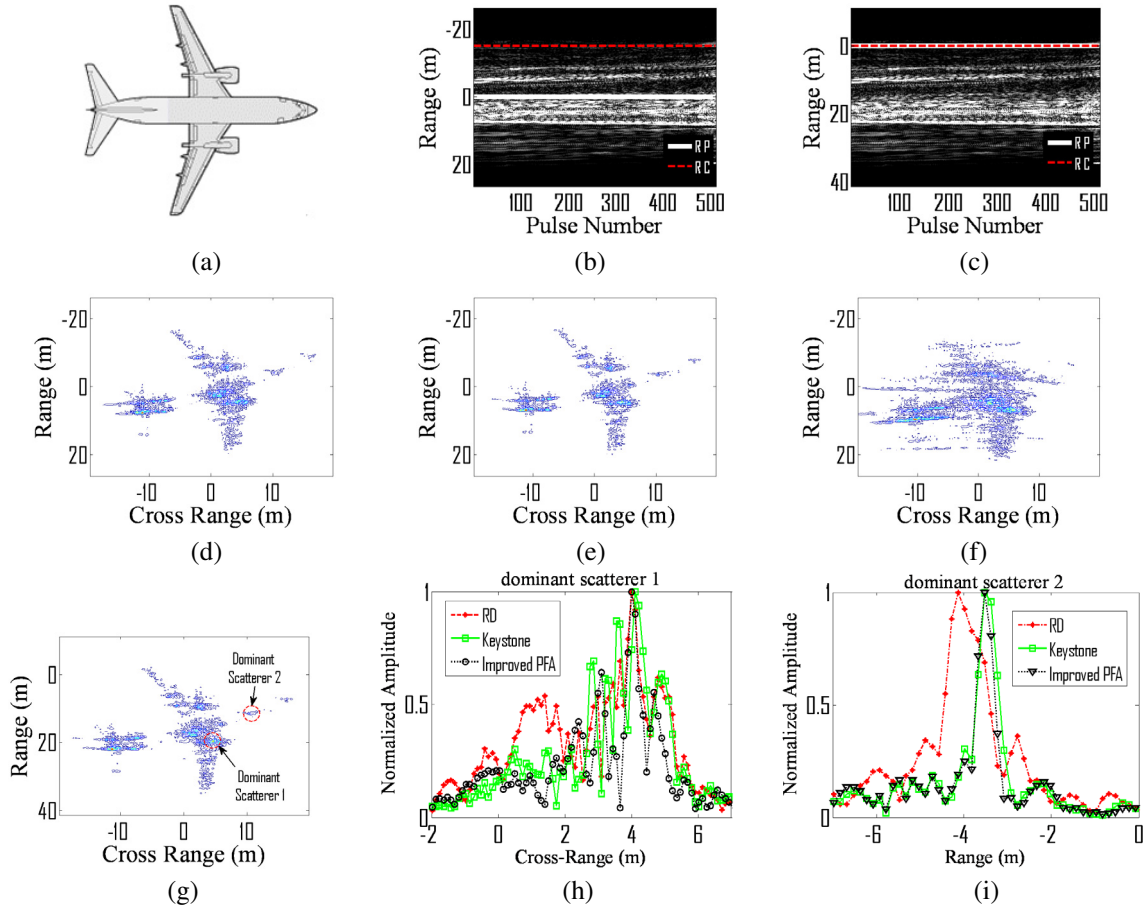
Figure 10. Real data experiment of Boeing 737. (a) Model of Boeing 737. (b) Original HRRPs. (c) HRRPs after range shift. (d) Image after RDA. (e) Image after Keystone algorithm. (f) ISAR image after traditional PFA. (g) ISAR image after impoved PFA. (h) PSF of scatterer 1 along cross-range dimension. (i) PSF of scatterer 2 along range dimension.

one utilizes PFA on the dechirped signals directly, the image is blurred in the cross-range direction. The HRRPS of shifted signals and the image after PFA interpolating are shown in Figs. 10(c) and(g), respectively. One can observe from Fig. 10(g) that more focused image was obtained by the proposed method. From Fig. 10(g), two dominant scatterers are chosen in range -19.6 m and -11.5 m. We plot the dominant scatterers corresponding to different algorithms respectively along cross-range and range dimensions in Figs. 10(h) and (i) in order to show the improvement on the point spread function (PSF) by the use of the improve PFA. From Figs. 10(h) and (i), we note that the blur caused by MTRC both in range and cross-range dimensions was compensated by the proposed method.

Moreover, we use image entropy and contrast value to evaluate the focused images in Fig. 10, which are presented in Table 1. It is notable in Table 1 that a well focused ISAR image was obtained by using the improved PFA.

Table 1. Entropy and contrast evaluation.

	RDA	Keystone	Traditional PFA	Improved PFA
Entropy	9.23	8.92	12.3	8.37
Contrast	6.32	6.57	4.23	7.04

5. CONCLUSION

The limitations of the traditional PFA algorithm for the dechirped echo signals in ISAR imaging is analyzed in this paper. The separation of RC and RP leads to the distributions of the 2-D scatterers mismatching the polar format. As a result, the image is blurred in the cross-range from PFA. In order to overcome the degradation, the RC in HIRRP is estimated by ICPF, and the dechirped signals after translational compensation are shifted in slant range accordingly. Consequently, the shifted signals follow the standard polar format. Experiments on simulated and real data show that the proposed method provides a promising performance improvement.

ACKNOWLEDGMENT

REFERENCES

1. Chen, C. C. and H. C. Andrews, "Target motion induced radar imaging," *IEEE Trans. Aerosp. Electron. Syst.*, Vol. 16, No. 1, 2–14, 1980.
2. Zhou, F., X. Bai, M. Xing, and Z. Bao, "Analysis of wide-angle radar imaging," *IET Radar, Sonar and Navigation.*, Vol. 5, No. 4, 449–457, 2011.
3. Xing, M., R. Wu, J. Lan, and Z. Bao, "Migration through resolution cell compensation in ISAR imaging," *IEEE Geosci. Remote Sens. Lett.*, Vol. 1, No. 2, 141–144, Apr. 2004.
4. Wang, Y. and Y. C. Jiang, "A novel algorithm for estimating the rotation angle in ISAR imaging," *IEEE Geosci. Remote Sens. Lett.*, Vol. 5, No. 4, 608–609, Oct. 2008.
5. Carrara, W. G. and R. S. Goodman, *Spotlight Synthetic Aperture Radar Signal Processing Algorithms*, 157–189, Artech House, Boston, MA, 1995.
6. LeCaillec, J.-M., "SAR remote sensing analysis of the sea surface by polynomial filtering," *IEEE Trans. Signal Process.*, Vol. 24, No. 4, 105–107, Jul. 2007.
7. Yu, T., M. D. Xing, and B. Zhen, "The polar format imaging algorithm based on double chirp-Z transforms," *IEEE Geosci. Remote Sens. Lett.*, Vol. 5, No. 4, 610–614, Oct. 2008.
8. Yang, Z. M., G. C. Sun, and M. D. Xing, "A new fast back-projection algorithm using polar format algorithm," *2013 Asia-Pacific Conference on Synthetic Aperture Radar*, 373–376, 2013.
9. Mensa, D. L., *High Resolution Radar Imaging*, 1224, Artech House, Dedham, MA, 1981.
10. Munoz-Ferreras, J. M. and F. Pérez-Martínez, "Uniform rotational motion compensation for inverse synthetic aperture radar with non-cooperative targets," *IET Radar Sonar Navig.*, Vol. 2, No. 1, 25–34, Jan. 2008.
11. Zhang, W. C., Z. P. Chen, and B. Yuan, "Rotational motion compensation for wide-angle ISAR imaging based on integrated cubic phase function," *IET International Radar Conference 2013*, Vol. 1, No. 5, 14–16. Apr. 2013.
12. Wang, M., A. K. Chan, and C. K. Chui, "Linear frequency-modulated signal detection using Radon-Ambiguity transform," *IEEE Trans. Signal Processing*, Vol. 46, No. 3, 571–586, Mar. 1998.
13. O'Shea, P., "A new technique for estimating instantaneous frequency rate," *IEEE Signal Processing Lett.*, Vol. 9, No. 8, 251–252, Aug. 2002.
14. Hu, J. M., W. Zhou, and Y. W. Fu, "Uniform rotational motion compensation for ISAR based on phase cancellation," *IEEE Geosci. Remote Sens. Lett.*, Vol. 8, No. 4, 636–641, Jul. 2011.
15. Wang, J., X. Liu, and Z. Zhou, "Minimum-entropy phase adjustment for ISAR," *IEE Proc. Radar Sonar Navig.*, Vol. 151, No. 4, 203–209, Aug. 2004.
16. Wang, J. F. D., "Kasilingam. Global range alignment for ISAR," *IEEE Trans. Aerosp. Electron. Syst.*, Vol. 39, No. 1, 351–357, 2003.